Punctual constraint resolution and deformation path on NURBS

Raphaël La Greca[*]
LSIS Laboratory

Romain Raffin[†]
LSIS Laboratory

Gilles Gesquière[‡]
LSIS Laboratory

Abstract

The Free From Deformations are the most spread methods to modify the shape of geometrical objects, described with vertices and faces. Many applications have been developed to extend this approach, allowing different constraint specifications or actions. It has also been adapted to deform subdivision or implicit surfaces. This paper introduces an improvement for NURBS surfaces, allowing a point picked on the surface to follow a curvilinear path. The principle of the method is to let the user choose a point on the NURBS surface and its destination location in space. Then, the deformation range and the curvilinear path from the constraint point to the displacement goal must be specified. The proposed process computes the deformation of the initial object to match a displacement constraint. In order to be applied on NURBS surfaces, the process uses the (u, v) parameters of the initial chosen point, but this computational step is hidden for the user.

CR Categories: I.3.5 [COMPUTER GRAPHICS]: Computational Geometry and Object Modeling—Curve, surface, solid, and object representations;

Keywords: Free Form Deformation, NURBS Surface, Constrained Deformation.

1 Introduction

Friendly deformation of parametric surfaces is still hard to obtain. Our work is focused on NURBS surfaces, and tends to insure the satisfaction of displacement constraint of points on the surface. These surfaces are widely used in CAD/CAM systems, because of their mathematic and geometric properties (weight usage, local basis and representation of the Bézier and B-Splines surfaces).

We can group the deformation methods of parametric surfaces into two parts: the soft constraints, generally interactively defined, which do not specify location or orientation constraints; the strict constraints imply the satisfaction of user, geometrical or mathematical constraints. This last part is complex and time-consuming for a design process but it insures the final object measures (size, orientation, tangency, ...). The "soft" methods permit to manipulate the parametric surface, moving control points or surface points (as in [Bartels and Beatty 1989], [Hsu et al. 1992]). They follow the user interaction but do not satisfy location constraint. For example, the user request can be a "rounded" surface but nothing defines precisely the final object characteristics.

In another branch of geometric modelling, some methods of deformation allow the user to fix constraints on a BREP mesh ([Borrel and Rappoport 1994] for instance). The user picks some points on the surface (it could be a mesh vertex or not), specifies a star-shaped range of influence, describes a path of deformation to each constraint and runs the deformation process which satisfies the user constraints. The influence hull is a restriction of the deformation

---
[*]e-mail: raphael.lagreca@lsis.org
[†]e-mail:romain.raffin@lsis.org
[‡]e-mail:gilles.gesquiere@lsis.org

toward the surface. Our goal is to combine a punctual deformation of NURBS surface with a path of deformation like in [Raffin 2000]. It will be interesting to model more complex forms.

In the first part of this paper, the principles of design scheme are recalled, the deformation methods are broached, first with FFD process and in the following part with the parametric surface model. In a fourth section, our model of deformation is described. Finally, after a conclusion on this work, some futures works will be proposed.

2 Design Scheme

The classical method used to design a complex surface in CAD/CAM is to define a surface (or a set of surfaces) only with equations, or to pick a simple surface and then deform it to obtain the desired one. The surface is often described by quadrics or parametric patches. As an example, the Figure 1 shows a car bonnet, defined as a parametric surface composed of a set of zones.
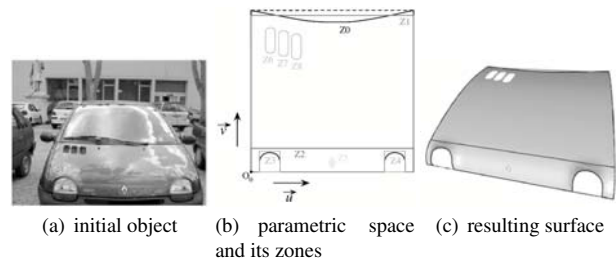

(a) initial object (b) parametric space and its zones (c) resulting surface

Figure 1: *Example of successive definitions of a complex parametric surface.*

The parametric surface is managed by a set of control points, the order of the polynomial basis used to link the resulting surface with these control points and the control points weight. The current methods to deform a parametric surface use multiresolution, physical or geometrical approaches.

The first one implies a wavelet description of the set of control points. Each level of resolution has an impact on the resulting surface, from a global range with a low resolution to some details addition for a full resolution [Kazinnik and Elber 1997]. The physical approaches are the most used to obtain intuitive reaction of the parametric surface. The first method has been due to [Terzopoulos et al. 1987]. It uses elasticity to model the reaction of the control points network. [Terzopoulos and Qin 1994] extend the NURBS model to D-NURBS (Dynamic) including mass and energy in the standard formulation of NURBS. This deformation model is based on Lagrangian dynamic. These two methods are time-consuming because they wish to reach a stable state for the complete network at each energy modification. On the same principle (but without modifying the NURBS definition), [Thingvold and Cohen 1990] propose a mechanical spring mass model matching the control points grid. [Léon and Trompette 1995] modify [Schek 1974] to implement a bars network linked with the control points. For a given set of intern or extern forces, the authors compute a stable solution satisfying various constraints (position, displacement, area, ...)

minimizing a choosen criterion (shape variation, area, ...) [Pernot 2004].

Even if these methods permit the deformation of a parametric surface, they are quite complex to be manipulated by a end user. We tend to base our work on geometrical methods, which can be more easily understood. The geometrical methods are other ways to deform parametric surfaces. Even if this deformation scheme is non exact, it can lead to intuitive tools for a end user ([Hsu et al. 1992] for instance). We propose to study a particular kind of method called Free Form Deformation which are developped in the next section.

3 Brief recall of Free Form Deformation methods

The Free Form Deformation method (FFD) has been designed to modify an object, whatever its representation: it acts on points (like in [Parent 1977]) and can be used to deform a surface or a volume. Primary works on Free Form Deformation were done by Sederberg and Parry [Sederberg and Parry 1986]. The principle of this model is quite simple. The object to be deformed is embedded in a parallelipipedical mesh (see Figure 2), deforming this mesh allows the deformation of the initial object.

Figure 2: *Example of a FFD applied on a teapot. Middle image, the teapot is embedded in a parallelipipedical mesh. Right, deforming the embedding volume implies the deformation of the teapot.*

Coquillard modified this model and proposed the extended FFD [Coquillart 1990] to use general prismatic meshes. Despite several extensions (proposed by [Moccozet and Magnenat-Thalmann 1997] and [Hsu et al. 1992]), the manipulation and the specification of the deformation range are not intuitive. The main drawback of FFD methods is that the user has to deform the mesh, without a direct control of the object surface. [Borrel and Bechmann 1991] implement a *n* dimensional deformation model (*DOGME*) which permits the satisfaction of constraints in the deformation. Using this, [Borrel and Rappoport 1994] create the *SCODEF* model which allows the user more interactivity with the deformation, adding a radius of influence to each constraint.

These two methods propose a deformation model which uses a punctual constraint with a given displacement (vector). An influence sphere (which radius can be modified) is linked to the punctual constraint. The method insures the satisfaction of the displacement constraint. [Raffin 2000] improves the *SCODEF* model with various hulls of influence, curve-constraint and deformation path. We will use this deformation model for the work which is described in this paper. In the following part, the definition of this model will be described.

As a Free Form Deformation model, *SCODEF* deforms the whole space an object is embedded in. The displacement of a point *P* submitted to *N* constraints in space is expressed as follows:

$$d(P) = M.f(P) \qquad (1)$$

with:

- *M* is the self-influence matrix, constructed with eq. 1 and all constraints,

- *f* is the deformation function linked to each constraint. The expression of f_i for the constraint *i* is:

$$f_i = B_i \left(\frac{\|C_i - P\|}{R_i} \right)$$

B_i is a B-Spline basis function, C_i is the constraint point and R_i its associated radius of influence.

- $d(C_i)$ is the displacement defined for each constraint point C_i.

A radius of influence R_i is linked to each constraint and allows the control of the locality of the deformation. The simple image in two dimensions of Figure 3 shows an object (an horizontal line) deformed by a *SCODEF* constraint. A constraint point is fixed and a displacement is given. The deformation acts only in the radius of influence. The deformation function used by the *SCODEF* model is a B-Spline basis function: the influence decreases when the distance between the constained point C_i and a given point *P* increases. When the distance is greater than the radius R_i, the influence of this constraint vanishes. The deformation function is centered at the constraint point (with the maximum value 1), it implies the displacement satisfaction. The resulting curve looks like a cubic B-Spline interpolation.
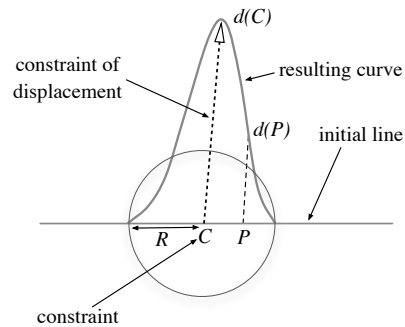

Figure 3: SCODEF *deformation sample of a line. Influence is circular.*

The *SCODEF* model provides an isotropic influence for a constraint. Influence area can be extended, keeping in mind that it is necessary to compute the distance between all points in the hull of influence and the constraint point. A solution is to use a star-shaped hull of influence, thus the influence hull can be non-convex but star-shaped and a distance between a point in the hull and the constraint point can always be computed.

As the *SCODEF* model provides straight vectors of displacement, the deformation cannot create bows or handles. Curvilinear displacements have been defined to allow this ([Raffin et al. 1999]). It implies to propose an other deformation function $f(P)$. For example, the deformation path can be represented by a Bézier curve, the parameter of this curve is the distance between the constraint point C_i and the point *P* in space, inducing that the constraints are not only punctuals but also curvilinear (see Figure 4 for various examples).
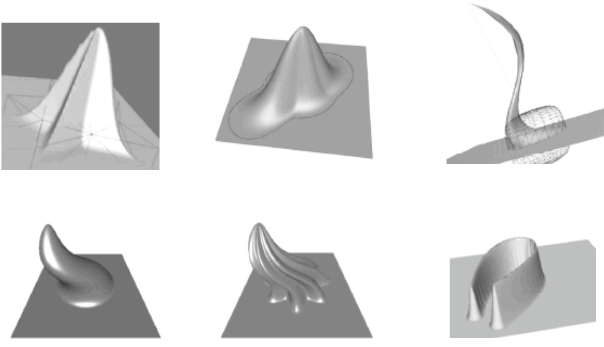
Figure 4: *Deformations obtained with an extended* SCODEF *method.*

4 Extension of surface deformation

Surface models are used in CAD. It would be important to bring tools to deform interactively this kind of surfaces. For example, Figure 5 shows some deformations of parametric surfaces, with various goals: to make a hole or to bulge, to extrude or to fold the surface. These deformations are defined to modify the control points or to use the parametric space (restriction of a hole for instance). These deformations are defined on NURBS surfaces that are introduced in the following section.
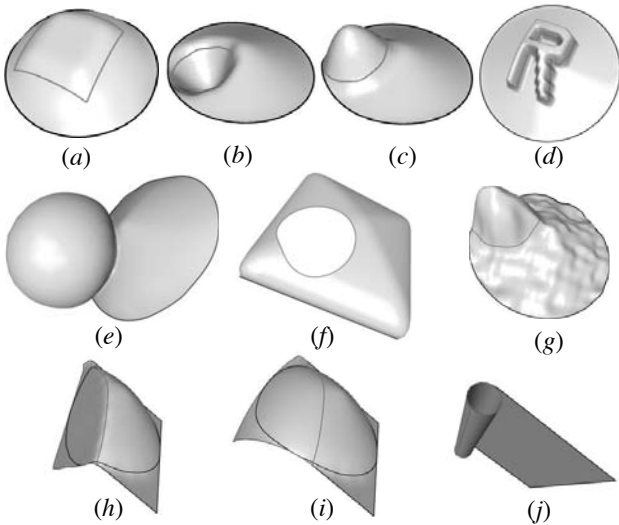

Figure 5: *Example of parametric surface deformations, acting on control points or parametric space (case of restriction).*

4.1 Notation

Giving S, a NURBS surface [Piegl and Tiller 1997] of degree p in the direction of u and degree q in the direction of v (cf Figure 6). A point of S with parameters $(u, v) \in D$ is computed with:

$$S(u,v) = \sum_{i=0}^{n-1}\sum_{j=0}^{m-1} R_{i,j}\mathbf{P}_{i,j}$$

with:

$$R_{i,j}(u,v) = \frac{N_{i,p}(u)N_{j,q}(v)w_{i,j}}{\sum\limits_{k=0}^{n-1}\sum\limits_{l=0}^{m-1} N_{k,p}(u)N_{l,q}(v)w_{k,l}}$$

Where:

- D is the definition domain of the parameters u and v. It is a parametric space given by $[0,1]^2$;

- $\{n\}$ and $\{m\}$ represent the number of control points in the u and v directions ;

- $\{P_{i,j}\}$ is the control point (i,j) ;

- $\{w_{i,j}\}$ is the weight of the control point $P_{i,j}$ with $\{w_{i,j}\} > 0$;

- $\{N_{i,p}(u)\}$ and $\{N_{j,q}(v)\}$ are the B-Spline basis of degree p and q defined on non decreasing sequences of knots U and V:

$$\begin{cases} U = \{U_0, \ldots, U_{p+n}\} & \text{with} \quad \forall i \in [0, p+n-1] \quad U_i \leqslant U_{i+1} \\ V = \{V_0, \ldots, V_{q+m}\} & \text{with} \quad \forall j \in [0, q+m-1] \quad V_j \leqslant V_{j+1} \end{cases}$$
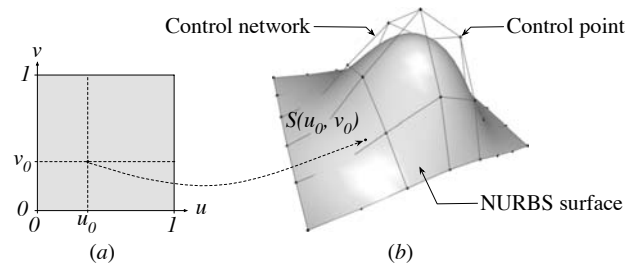

Figure 6: *(a) Parametric space D. (b) NURBS surface defined on D.*

4.2 Satisfaction of a linear punctual constraint

The surface deformation presented in previous section will be applied on NURBS surface. We present now a new deformation tool on NURBS. We wish to satisfy linear punctual constraints. Let $\hat{M}$ be a point in space and M a point of the parametric surface S, with $M = S(u,v)$, the goal of the method is to deform S to obtain a surface $\hat{S}$ verifying $\hat{S}(u,v) = \hat{M}$ (see Figure 7). A deformation constraint is denoted G ($[M\hat{M}]$ segment in the figure) and defined by:

1. a spatial constraint: the resulting surface $\hat{S}$ must go through $\hat{M}$;

2. a parametric constraint: the point of $\hat{S}$ matching with $\hat{M}$ must have parameters pair (u,v) ;

3. a localization constraint: each constraint has an influence on S, defined by the function $f(i,j)$:

$$\begin{cases} f : [0, n-1] \times [0, m-1] \mapsto \mathbb{R}^+ \\ \exists (i,j) \in [0, n-1] \times [0, m-1] \,/\, R_{i,j}(u,v)f(i,j) \neq 0 \end{cases}$$

When $f(i,j) = R_{i,j}(u,v)$, G has a "natural" influence on the surface.

The solving method [La Greca 2005] is geometrically based. It consists in the modification of the control point $P_{i,j}$, defining the surface S, with a displacement computed according to eq. (2).
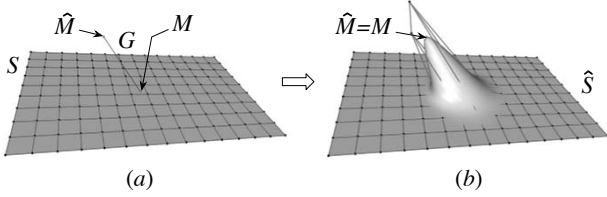
Figure 7: *(a) A surface S of degree 3×3, defined by 15×10 control points. G is the constraint to satisfy (natural influence). (b) Resulting surface $\hat{S}$.*

$$\overrightarrow{m(i,j)} = \frac{f(i,j)}{\displaystyle\sum_{k=0}^{n-1}\sum_{l=0}^{m-1}[R_{k,l}(u,v)f(k,l)]} \overrightarrow{e} \quad \text{with } \overrightarrow{e} = \overrightarrow{M\hat{M}} \quad (2)$$

The Figure 8 shows the influence impact of G when the natural influence is enlarged by gaussian convolution of radius $\hat{n}$. We can select some points in the parametric space to modify their locations. The influence zone remains isotropic (disc on intial surface).
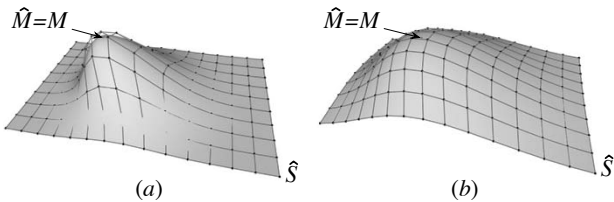

Figure 8: *Resulting surface satisfying G with $\hat{n} = 10$ (a) and $\hat{n} = 20$. (b) as filter size of the gaussian convolution.*

The $f(i,j)$ function can directly be given by the designer as a zone on the surface. This method of description is more intuitive for the user who does not have to know the underlying mathematical model. Indeed, he or she has just to "draw" on the surface the zone to deform. The zone can also be represented in the parametric space. In this case it is called the *parametric zone* or the *parametric image* of the zone, as illustrated in Figure 9. In addition, it is important to note that a parametric zone must include the parametric constraint (u,v) of the G constraint to satisfy.
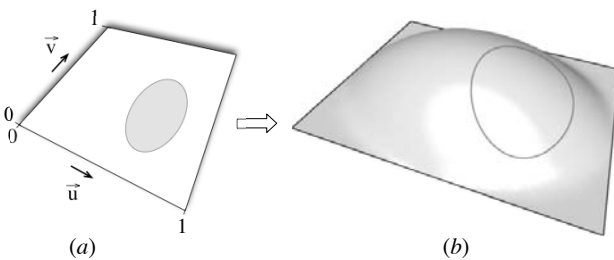

Figure 9: *(a) Representation of a zone in the parametric space (parametric image of the zone), (b) corresponding shape drawn on the surface.*

If the deformation needs more control points, in case of a small zone for instance, the control grid has to be refined by adding lines and columns of control points inside the zones which have to be deformed. This operation can be done using the knots insertion

algorithm developed by Boehm [Boehm and Prautzsch 1985] for example.

The influence $f(i,j)$ of the constraint linked to the zone has now to be determined according to the needed deformation. To do this, we introduce the notion of *parametric image of a control point $P_{i,j}$* [La Greca 2005] which is the (u_i, v_j) pair such as $P_{i,j}$ is the control point with the biggest influence on $S(u_i, v_j)$. The method to find all these parametric images uses a flat surface $\tilde{S}$ defined by the same features (degrees, knots vectors) than the surface S to be deformed. The (u_i, v_j) pairs are the parameters of the points of $\tilde{S}$ matching with the control points $\tilde{P}_{i,j}$ of $\tilde{S}$ such as: $\tilde{S}(u_i, v_j) = \tilde{P}_{i,j}$.

The influence $f(i,j)$ is then found by the following: the control points of the surface which *parametric images* are outside the parametric zone are considered as fixed during the deformation ($f(i,j) = 0$). The other control points are related to an influence value equal to $f(i,j)$. A good way to initialize $f(i,j)$ is to choose a high value when the *parametric image* of $P_{i,j}$ is close, in the parametric space, to the parametric constraint (u,v) to satisfy. A low value is chosen when the *parametric image* of $P_{i,j}$ is close, in the parametric space, to the border of the parametric zone. The Figure 10 illustrates this step showing two zones with different levels of refinement.
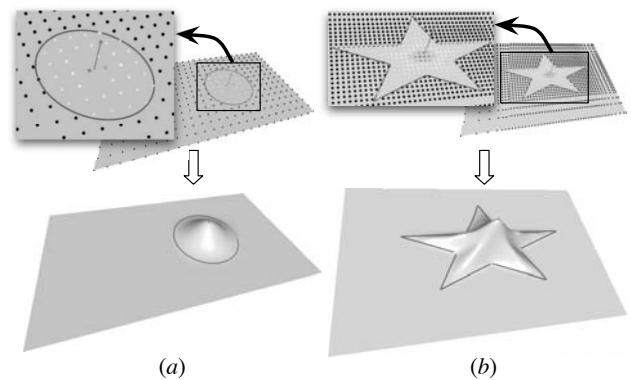

Figure 10: *Definition of the influence of a constraint from a zone of the surface. Two levels of refinement (a) and (b) of the control grid are illustrated using two different shapes of zone. The dark control points outside the zone are fixed, the mobile ones are inside the zone and colored according to their influence $f(i,j)$ from light for a low influence to dark for a high one.*

As in the previous work in BREP mesh of [Raffin et al. 1999], it would be interesting to replace the direct line path by a 3D curve to deform the surface from the constraint point to the goal one. The next section explains this new deformation process.

4.3 Satisfaction of a path constraint

We propose to add to the previous definition of a constraint G (Cf. 4), a fourth sub-constraint which is a curve path the surface has to follow during its deformation. Thus, a punctual constraint G is now defined by a spatial constraint, a parametric constraint, a localization constraint and a *path constraint* as illustrated in Figure 11. This path is given by a NURBS curve $C(t)$ with $t \in [0; 1]$. It must have a clamped knots vector in order to ensure $M = C(0)$ and $\hat{M} = C(1)$. These two equalities define the relationship between the path constraint and the surface before and after its deformation.
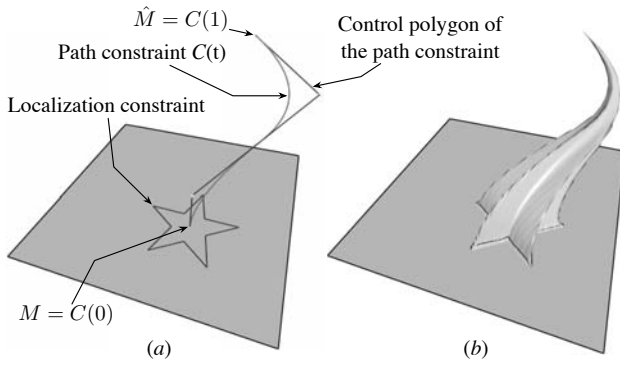
Figure 11: *Definition of a path constraint (a) and its satisfaction (b).*

This kind of constraint can be used to allow the user to satisfy a punctual constraint avoiding a place or a volume in space for instance. The process we introduce to satisfy it, is an iterative deformation of the surface following the parametric curve $C(t)$. This curve is steadily sampled and viewed as a set of N segments. We choose N as ten times the product of the degree of $C(t)$ per its number of control points, this sampling technique gives good visual results but produces many steps. One future work is to find an optimal sampling method taking into consideration the curvature of C for example.

One step $k \in [0, N-1]$ of our method consists in viewing the k-segment as a linear punctual constraint defined by $\vec{e_k} = \overrightarrow{C(\frac{k}{N})C(\frac{k+1}{N})}$. The satisfaction of this constraint is done at each step applying the equation (2) where the error vector $\vec{e}$ is equal to $\vec{e_k}$.

However, if the localization constraint used is the same throughout the process, the resulting surface is the same as the surface satisfying the linear punctual constraint defined by $\overrightarrow{M\hat{M}}$. Indeed, in this case, the sum of all the segments is equal to $\overrightarrow{M\hat{M}}$ by the parallelogram relation, that is why we choose to reduce the localization constraint at each step of the method: the more the step is close to $N-1$, the more the localization constraint is reduced.

In practice, we consider that the localization constraint $f(i, j)$ of G is normalized in order to use $f(i, j) \in [0, 1] \ \forall (i, j) \in [0, n-1] \times [0, m-1]$. The control points $P_{i,j}$ involved in the deformation ($f(i, j) > 0$) make a set written L. Then, our idea is to define a new influence $\tilde{f}_k(i, j)$ at each step of the process according to the $f(i, j)$ localization and a threshold $s(k) \in [0, 1]$ which is linearly defined as $s(k) = \frac{k}{N-1}$. This new influence is computed such as:

$$\tilde{f}_k(i, j) = \begin{cases} \begin{cases} 0 & \text{if } f(i, j) < s(k) \\ \begin{cases} f(i, j) & \text{if } k = N-1 \\ 1 & otherwise \end{cases} & otherwise \end{cases} \end{cases} \quad (3)$$

For each $\tilde{f}_k(i, j) > 0$, it can be associated a set L_k of control points involved in the deformation during the step k. This new influence (3) used with equation (2) is equivalent to translate by $\vec{e_k}$ all the control points $P_{i,j}$ where $f(i, j) \geqslant s(k)$ and $k < N-1$. This technique could be viewed as to spread the surface along the curved path. Finally the last step ($k = N-1$) really satisfies the punctual constraint using (2) with a small localization constraint defined by a few set of control points L_{N-1}. Figure 12 shows the impact of

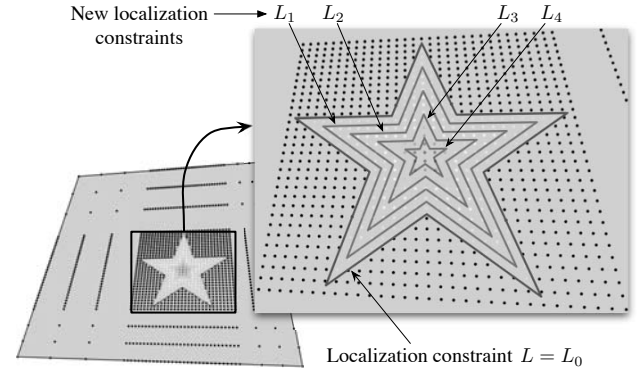the evolution of the threshold $s(k)$ on the sets of control points (L_k) involved in this deformation process.

Figure 12: *Example of evolution of the shape of a localization constraint during a process of 5 steps ($N = 5$).*

One implication of the evolution of the shape of the localization constraint during the process is the need of many control points. Indeed, the more the number of segments N is large, the more the number of steps increases and the more the need of control points in the zone is important. That is why the refinement of the control network of S depends on N and on the shape of the localization constraint. We currently add a sufficient number of control points which is most of the time very large. One very important future work is to develop a precise refinement technique to minimize this number of control points.

In order to follow the path constraint, the more natural way is to drive the deformation with the tangent of C. In our case, each segment $\vec{e_k}$ of the sampled path can be considered as the direction to follow (see Figure 13). That is why in addition to the translation e_k, a rotation is applied to each $P_{i,j} \in L_k$ in order to satisfy the direction of deformation. This rotation is defined by two data:

- The angle α_k made by the two consecutive segments $\vec{e_k}$ and $\overrightarrow{e_{k+1}}$.
- The axe going through $C(\frac{k}{N})$ and carried by $\vec{e_k} \wedge \overrightarrow{e_{k+1}}$, that is orthogonal to the plane defined by $\vec{e_k}$ and $\overrightarrow{e_{k+1}}$.
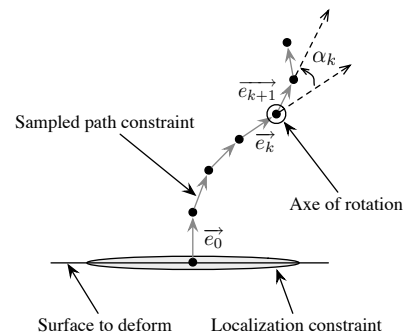

Figure 13: *Set of segments illustrating the sampled path constraint and angle α defined by two successive segments.*

Figure 14 illustrated two different steps of the process and its result on a B-Spline surface with a star-shaped localization constraint. Figure 15 presents an other result of a curve path deformation applied on a B-Spline surface with an influence defined by a circular-shaped zone.
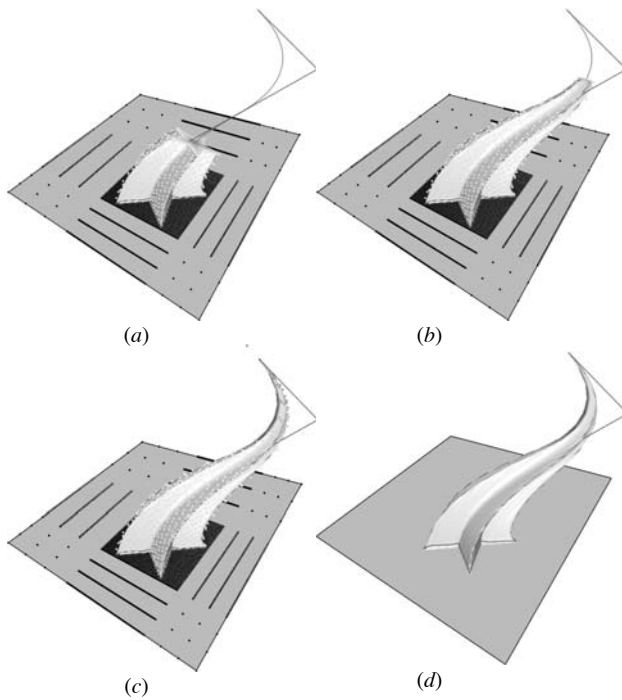
(a)   (b)

(c)   (d)

Figure 14: *Two steps in (a) and (b) of the satisfaction of a path constraint illustrated in (c) and (d) (80 steps, 240 ms - PowerPC 1.33 Ghz - 768 Mo RAM).*

5 Conclusion and futures works

As in the previous work in BREP mesh of [Raffin et al. 1999], we implement a 3D path of deformation to pull the surface from the constraint point to a goal point. The principle resides in the step by step deformation of the surface, following a parametric curve defined from the constraint point. We have shown that a direct displacement can be easily satisfied, an we can subsequently sample a 3D curve in segments that can be satisfied and provide a path of deformation to constrained surface deformation. This method permits new deformation types on NURBS surfaces, according to the user needs.

We proposed many improvements: first the generic deformation function which allows the modification of the object shape interactively ; the hull of influence which rules the locality and the shape
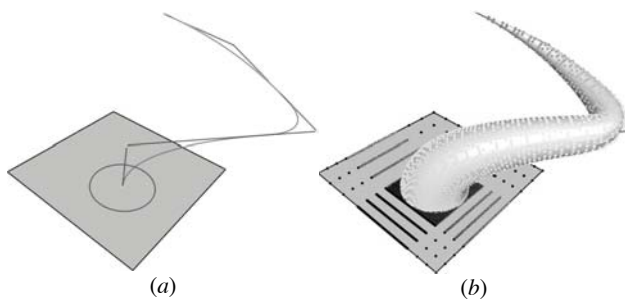

(a)   (b)

Figure 15: *Example of a constrained path with a circular-shaped localization constraint in (a) and its satisfaction in (b) (100 steps, 420 ms - PowerPC 1.33 Ghz - 768 Mo RAM).*

of the deformation; and the curvilinear displacement or constraint path that allows a wide range of deformations. All these contributions are independents from each other and do not change the basis of the deformation or the NURBS expression. Thus, we can combine any functions of deformation with any hull of influence and any curvilinear displacement.

The futures works we plan are the extension of the path constraint to curvilinear constraints and a better management of local differential parameters in order to create profilers of the deformation. We also need to manage efficiently the knots insertion in order to avoid unused control points and the important growth memory it carries. As a constraint is linked to an influence zone, we must only refine the control grid in this area. Another part of reflexion is the adaptation of this model to deform a surface with constraints made of curve or surface.

References

BARTELS, R., AND BEATTY, J. 1989. A technique for the direct manipulation of spline curves. *Graphics Interface*, 33–39.

BOEHM, W., AND PRAUTZSCH, H. 1985. The insertion algorithm. *Computer-Aided Design 17*, 2, 58–59.

BORREL, P., AND BECHMANN, D. 1991. Deformation of ndimensional objects. *International Journal of Computational Geometry and Applications 1*, 4, 427–453.

BORREL, P., AND RAPPOPORT, A. 1994. Simple constrained deformations for geometric modeling and interactive design. *ACM Transactions on Graphics 13*, 2, 137–155.

COQUILLART, S. 1990. Extended free-form deformation: A sculpturing tool for 3d geometric modeling. *Computer Graphics (ACM SIGGRAPH Proceedings) 24*, 4, 187–196.

HSU, W., HUGHES, J., AND KAUFMAN, H. 1992. Direct manipulation of free-form deformations. *Computer Graphics (ACM SIGGRAPH Proceedings) 26*, 2, 177–184.

KAZINNIK, R., AND ELBER, G. 1997. Orthogonal decomposition of non-uniform b-spline spaces using wavelets. *Computer Graphics Forum 16*, 3, 27–38.

LA GRECA, R. 2005. *Approche déclarative de la modélisation de surfaces*. Phd thesis, Université de la Méditerranée.

LÉON, J.-C., AND TROMPETTE, P. 1995. A new approach towards free-form surfaces control. *Computer Aided Geometric Design 12*, 395–416.

MOCCOZET, L., AND MAGNENAT-THALMANN, N. 1997. Dirichlet free-form deformations and their application to hand simulation. In *Proceedings Computer Animation 97, IEEE Computer Society*, 93–102.

PARENT, R. E. 1977. A system for sculpting 3-d data. In *SIGGRAPH '77: Proceedings of the 4th annual conference on Computer graphics and interactive techniques*, ACM Press, New York, NY, USA, 138–147.

PERNOT, J.-P. 2004. *Fully Free Form Deformation Features for Aesthetic and Engineering Designs*. Phd thesis, Institut National Polytechnique de Grenoble.

PIEGL, L., AND TILLER, W. 1997. *The NURBS Book 2nd Edition*. Springer, Berlin.

RAFFIN, R., NEVEU, M., AND JAAR, F. 1999. Curvilinear displacement of free-from based deformation. *The Visual Computer 16*, 38–46. Springer-Verlag Editions.

RAFFIN, R. 2000. *Generalised constrained deformations (in French)*. Phd thesis, Université de Bourgoge.

SCHEK, H. J. 1974. The force density method for form-finding and computation of general networks. *Computer Methods in Applied Mechanics and Engineering 3*, 2, 115–134.

SEDERBERG, T., AND PARRY, S. 1986. Free-form deformation of solid geometrics models. *ACM Transactions on Graphics 20*, 4, 151–160.

TERZOPOULOS, D., AND QIN, H. 1994. Dynamic nurbs with geometric constraints for interactive sculpting. *ACM Transactions on Graphics 13*, 2, 103–136.

TERZOPOULOS, D., PLATT, J., BARR, A., AND FLEISCHER, K. 1987. Elastically deformable models. *Computer Graphics (ACM SIGGRAPH Proceedings) 21*, 4, 205–214.

THINGVOLD, J. A., AND COHEN, E. 1990. Physical modeling with b-spline surfaces for interactive design and animation. In *Symposium on Interactive 3D graphics*, ACM Press, 129–137.